TAO, Vol.5, No.1, 43-62, March 1994

A Cloud Chemistry Model: Simulation of Cloud Water Acidity and Its Dependence on Droplet Size

NENG-HUEI LIN[1]

(Manuscript received 28 December 1993, in final form 7 March 1994)

ABSTRACT

The purpose of this study is to investigate the possible chemical pathways determining the acidity and chemical composition of cloud water and the role played by individual cloud droplets. A kinetic cloud chemistry model (CCM) involving the aqueous phase chemistry of sulfur species and aerosol loadings is developed for a modeling approach. The solution chemistry involves SO_2, HNO_3, HCl, NH_3, CO_2, O_3 and H_2O_2 gases and the oxidation of S(IV) by O_3 and H_2O_2. The scavenging of acidic (H_2SO_4), neutral ($(NH_4)_2SO_4$ and NH_4NO_3), maritime (NaCl and KCl), and continental ($CaCO_3$ and $MgCO_3$) aerosols are included in CCM. A scheme is developed to investigate the dependence of the acidity and chemical composition in cloud droplets upon their sizes. Using the Khrgian-Mazin droplet size distribution, the model simulations show that contrary to expectations, smaller droplets have higher pH values although the sulfate ion concentrations in them are much higher than in larger droplets. This seems to result from the loadings of carbonate aerosols. If the latter is excluded, the pH value for the smallest droplet can be even below 2.0. The variation of pH with size for larger droplets is not significant. The acidity in smaller droplets is most sensitive to the mass loading of aerosol particles. The dilution effect in larger droplets is clearly seen. The model results are compared with direct measurements made in clouds at Mt. Mitchell, NC. The data on cloud water acidity with a temporal resolution of about 10 min are available. Cloud droplet size distribution was simultaneously measured using Forward Scattering Spectrometer Probe (FSSP). A case study comparing the model results with the observations is presented and the dependence of the chemical composition of cloud water upon droplet size is analyzed. A qualitative agreement between the model predictions and direct observations is found.

(Key words: Cloud chemistry model, Cloud water acidity, Sulfurchemistry)

[1] Department of Atmospheric Sciences, National Central University, Chung-Li, Taiwan, R.O.C.

1. INTRODUCTION

The chemical composition of atmospheric aerosols varies significantly with size (Pruppacher and Klett, 1980). Aerosol properties evolve due to chemical reactions, nucleation, and growth by molecular diffusion and coagulation (Lee, 1983). Subsequently, cloud droplets form on the condensation nuclei whose water solute portion is primarily composed of sulfate, nitrate and other species. During the cloud droplet spectral evolution, the chemical properties and resulting acidity will change due to molecular diffusion of pollutant gases into droplets, and the coagulation between droplets of different sizes and chemical composition (Lee, 1986). The above size dependency of cloud acidity and chemical composition in clouds will alter the overall air pollution budget in a region containing clouds. Therefore, clouds play an important role of removing and redistributing the atmospheric pollutants (Saxena and Lin, 1990; Lin and Saxena, 1991a, b).

According to the experimental study conducted by Noone *et al.* (1988), the volumetric mean-solute concentration in cloud droplets of 9-18 μm sampled from a maritime stratus cloud was a factor of 2.7 smaller than that of cloud droplets of 18-23 μm. During the Po Valley Fog Experiment 1989 (Heintzenberg, 1992), The size dependence of the mass concentration of nonvolatile material in fog droplets was studied (Ogren *et al.*, 1992), indicating that the mass concentration decreases monotonically with droplet size over the entire observed range of 1 to 40 μm in diameter.

As for the modeling studies, using an entraining air parcel cloud model, Flossmann *et al.* (1985) suggested that the mass mixing ratio of aerosols is larger in smaller than larger drops when condensation and collision-coalescence are the dominant processes. On the contrary, other theoretical studies (Hegg and Hobbs, 1979; Jensen and Charlson, 1984) found that the total mass concentration of aerosols is smaller inside the smaller drops when nucleation scavenging is the controlling process. Hegg and Larson (1990) indicated that such size dependency may affect the sulfate production rate in the cloud. Pandis and Seinfeld (1990) found that during the period of dense fog, solute concentration in droplet diameters larger than 10 μm increases with size, and the growth factor is 3.6 for droplet diameters from 10 to 20μm.

In this paper, a diagnostic cloud chemistry model is developed to simulate the cloud acidity due to scavenging of aerosols and gases by cloud droplets in open and closed systems. A scheme is also developed to calculate the dependency of pH value and chemical composition in cloud droplets upon their sizes. The model is aimed at identifying and quantifying the effect of individual chemical processes on the final acidity of cloud droplets. The model simulations are also compared with the measurements performed during a cloud event at a remote mountain site.

2. CLOUD CHEMISTRY MODEL

The cloud chemistry model includes the absorption of trace gases, the oxidation of aqueous phase SO_2, and the scavenging of acidic (H_2SO_4), neutral ($(NH_4)_2SO_4$ and NH_4NO_3), maritime (NaCl and KCl), and continental ($CaCO_3$ and $MgCO_3$) aerosols. In this study, it is mainly considered that the solution chemistry involves the SO_2, HNO_3, HCl, NH_3, CO_2, O_3 and H_2O_2 gases and the oxidation of S(IV) (the oxidation state 4 of dissolved sulfur in solution) by O_3 and H_2O_2 (Schwartz, 1984). The relevant chemical reactions with the

equilibrium constants or rate expressions are listed in Tables 1-3 for the solubility processes, aqueous equilibrium expressions, and reactions of S(IV) oxidation, respectively. Easter and Luecken (1988) have also provided similar information.

It is assumed that all aerosols considered in this study are totally soluble within the aqueous phase, and as a result, at the instant of cloud formation, these are immediately incorporated into the aqueous phase (see Table 4).

2.1 Model Formulation for an Open System

In an open system, the gaseous concentrations are assumed to be constant. Based on chemical reactions considered in this study and the theory of electroneutrality, when equilibrium between gas and aqueous phases in cloud droplets is established, the concentrations of all ions in the liquid satisfy the following equation:

$$[H^+] + [NH_4^+] + [CAT^+] + 2[CAT^{2+}] = [OH^-] + [Cl^-] + [HSO_3^-] + 2[SO_3^{2-}] + 2[SO_4^{2-}] + [NO_3^-] + [HCO_3^-] + 2[CO_3^{2-}] \quad (1)$$

where CAT represents the dissolved but unreacted cations such as sodium, potassium, calcium, magnesium, and so on. The concentrations of the ions in liquid can be expressed in terms of $[H^+]$, for example,

$$[NH_4^+] = \frac{K_{ha}K_{a1}}{K_w}[H^+]p_{NH_3} \quad (2)$$

$$[OH^-] = \frac{K_w}{[H^+]} \quad (3)$$

$$[Cl^-] = \frac{K_{hl}K_{l1}}{[H^+]}p_{HCl} \quad (4)$$

$$[HSO_3^-] = \frac{K_{hs}K_{s1}}{[H^+]}p_{SO_2} \quad (5)$$

$$[SO_3^{2-}] = \frac{K_{hs}K_{s1}K_{s2}}{[H^+]^2}p_{SO_2} \quad (6)$$

$$[NO_3^-] = \frac{K_{hn}K_{n1}}{[H^+]}p_{HNO3} \quad (7)$$

$$[HCO_3^-] = \frac{K_{hc}K_{c1}}{[H^+]}p_{CO_2} \quad (8)$$

$$[CO_3^{2-}] = \frac{K_{hc}K_{c1}K_{c2}}{[H^+]^2}p_{CO_2} \quad (9)$$

In the above equations, K_{hx} is the Henry's law coefficient for the species x such as l for HCl, c for CO_2, s for SO_2, a for NH_3, n for HNO_3 and w for water; p_x is the gas concentration

Table 1. Solubility constants used in model computations.
(Units for solubility constants are mole l^{-1} atm^{-1})

Solubility process	Solubility constant	Reference*
$SO_{2(g)} \leftrightarrow SO_{2(aq)}$	$K_{hs} = [SO_{2(g)}]/[SO_{2(aq)}] = \exp(-10.25 + 3121.7/T)$	1
$CO_{2(g)} \leftrightarrow CO_{2(aq)}$	$K_{hc} = [CO_{2(g)}]/[CO_{2[aq]}] = \text{antilog}(-14.018 + 2385.7/T + 0.015264xT)$	2
$HNO_{3(g)} \leftrightarrow HNO_{3(aq)}$	$K_{hn} = [HNO_{3(g)}]/[HNO_{3(aq)}] = \exp(3659/T)$	3
$HCl_{(g)} \leftrightarrow HCl_{(aq)}$	$K_{hl} = [HCl_{(g)}]/[HCl_{(aq)}] = 1540$	4
$NH_{3(g)} \leftrightarrow NH_{3(aq)}$	$K_{ha} = [NH_{3(g)}]/[NH_{3(aq)}] = 12.187/T \text{ antilog}(-1.69 + 1477.7/T)$	5
$H_2O_{2(g)} \leftrightarrow H_2O_{2(aq)}$	$K_{hh} = [H_2O_{2(g)}]/[H_2O_{2(aq)}] = \exp(-12.24 + 6981.6/T)$	6
$O_{3(g)} \leftrightarrow O_{3(aq)}$	$K_{ho} = [O_{3(g)}]/[O_{3(aq)}] = 1.402x10^{-5} \exp(2013.1/T)$	7

* 1: Hales and Sutter, 1973; Johnstone and Leppla, 1934;
2: Harned and Davis, 1943;
3: Schwartz and White, 1981;
4: Chen *et al.*, 1979, temperature dependence uncertain, assumed constant;
5: Hales and Drews, 1979;
6: Martin and Damschen, 1981;
7: Wagman *et al.*, 1968.

Table 2. Aqueous equilibrium expressions used in model computation.
(Unit: mole l^{-1}(M), unless otherwise noted.)

Equilibrium process	Equilibrium constant	Reference*
$SO_{2(aq)} \leftrightarrow H^+ + HSO_3^-$	$K_{s1} = [H^+][HSO_3^-]/[SO_{2(aq)}] = \exp(-10.965 + 1972.4/T)$	1
$HSO_3^- \leftrightarrow H^+ + SO_3^{2-}$	$K_{s2} = [H^+][SO_3^{2-}]/[HSO_3^-] = \exp(-23.14 + 1954.7/T)$	2
$CO_{2(aq)} \leftrightarrow H^+ + HCO_3^-$	$K_{c1} = [H^+][HCO_3^-]/[CO_{2(aq)}] = \text{antilog}(14.8435 - 3404.71/T - 0.032786xT)$	3
$HCO_3^- \leftrightarrow H^+ + CO_3^{2-}$	$K_{c2} = [H^+][CO_3^{2-}]/[HCO_3^-] = \text{antilog}(6.498 - 2902.39/T - 0.02379xT)$	3
$HNO_{3(aq)} \leftrightarrow H^+ + NO_3^-$	$K_{a1} = [H^+][NO_3^-]/[HNO_{3(aq)}] = \exp(815.3/T)$	4
$HCl_{(aq)} \leftrightarrow H^+ + Cl^-$	$K_{l1} = 6310$	5
$NH_{3(aq)} \leftrightarrow OH^- + NH_4^+$	$K_{a1} = [OH^-][NH_4^+]/[NH_{3(aq)}] = K_w \text{antilog}(0.09018 + 2729.92/T)$	6
$H_2O \leftrightarrow H^+ + OH^-$	$K_w = [H^+][OH^-] = \text{antilog}(-4.098 - 3245.2/T - 2.2362x10^5/T^2 - 3.984x107/T^3)$ (M^2)	7

* 1: Hales and Sutter, 1973; Johnstone and Leppla, 1934;
2: Weast, 1984; Beilke and Gravenhorst, 1978;
3: Harned and Davis, 1943;
4: Schwartz and White, 1981; Wagman *et al.*, 1968;
5: Cruz and Rennon, 1978, temperature dependence uncertain, assumed constant;
6: Hales and Drews, 1979;
7: Weast, 1984.

Table 3. Aqueous chemical reactions used in model computation. (Units are mole l^{-1}(M) for aqueous concentrations and M s^{-1} for reaction rates.

Reaction	Reaction Rate	Reference*
$S(IV) + H_2O_{2(aq)} \rightarrow SO_4^{2-}$	$d[SO_4^{2-}]/dt = 8.3\times10^4[H_2O_{2(aq)}][SO_{2(aq)}]/(0.1+[H^+])$	1
$S(IV) + O_{3(aq)} \rightarrow SO_4^{2-}$	$d[SO_4^{2-}]/dt = (k_1[HSO_3^-] + k_2[SO_3^{2-}])[O_{3(aq)}]$	
	$k_1 = \exp(33.33 - 6140/T)$ $k_2 = \exp(41.67 - 6000/T)$	2

* 1: Martin and Damschen, 1981;
2: Erickson *et al*, 1977.

Table 4. Aerosol particles are assumed to be 100% dissolved into the cloud droplets.

$H_2SO_{4(s)} \rightarrow 2H^+ + SO_4^{2-}$
$(NH_4)_2SO_{4(s)} \rightarrow 2NH_4^+ + SO_4^{2-}$
$NH_4NO_{3(s)} \rightarrow NH_4^+ + NO_3^-$
$NaCl_{(s)} \rightarrow Na^+ + Cl^-$
$KCl_{(s)} \rightarrow K^+ + Cl^-$
$CaCO_{3(s)} \rightarrow Ca^{2+} + CO_3^-$
$MgCO_{3(s)} \rightarrow Mg^{2+} + CO_3^-$

of species x; $K_{xi}$is the dissociation equilibrium constant for species x; subscript i denotes the order of dissociation. By replacing the ion concentrations in Eq. (1), except the $[H^+]$ with the relationship expressed in Eqs. (2)-(9), a cubic equation of $[H^+]$ is formed as follows.

$$A[H^+]^3 + B[H^+]^2 + C[H^+] + D = 0\,, \tag{10}$$

where A, B, C and D are the function of the above p_x and k_x. These coefficients can be expressed by

$$A = 1 + \frac{K_{ha}K_{a1}p_{NH_3}}{K_w}\,, \tag{11}$$

$$B = [CAT^+] + 2[CAT^{2+}] - 2[SO_4^{2-}]\,, \tag{12}$$

$$C = -(K_{hl}K_{l1}p_{HCl} + K_{hs}K_{s1}p_{SO_2} + K_{hn}K_{n1}p_{HNO_3} + K_{hc}K_{c1}p_{CO_2} + K_w)\,, \tag{13}$$

and

$$D = -2(K_{hs}K_{s1}K_{s2}p_{SO_2} + K_{hc}K_{c1}K_{c2}p_{CO_2}). \quad (14)$$

In Eq. (12), the sulfate ion concentration is calculated as follows.

$$[SO_4^{2-}]_t = [SO_4^{2-}]_{t-\Delta t} + \left(\frac{d[SO_4^{2-}]}{dt}\right)_{t-\Delta t} \Delta t\ , \quad (15)$$

where Δt is the integrated time. According to the oxidation rate of S(IV) ($[SO_2(aq)]+[HSO_3^-]+[SO_3^{2-}]$) by O_3 and H_2O_2 as listed in the Table 3, the rate of change of $[SO_4^{2-}]$ can be computed. Thus, Eqs. (2)-(10) are solved iteratively for $[H^+]$ for each time step. The iteration is stopped when the absolute error of two consecutive pH values is within the error limit (in this study, the error limit is 0.001). The other ionic concentrations are then calculated based on Eqs. (2)-(9).

2.2 Model Formulation for a Closed System

In a closed system, for an air parcel without mass exchange with the environment, the total concentrations of these gases in both gaseous and aqueous phases are assumed invariable. This is a good assumption when the air parcel is regarded as a reactive chamber and the relative importance of chemical reactions involved can be investigated. If p_x° represents the initial gaseous concentration and q_x is the aerosol mass concentration of species x, the following relationship shows the conservation of the mass for species x when it dissolves into cloud droplets (Walcek and Taylor, 1986):

$$p_x^0 + \frac{q_x RT}{M_x} = p_x + [(x)]LRT\ , \quad (16)$$

where L, R and T are the cloud liquid water content (LWC), the universal gas constant and the temperature of cloud droplets, respectively. Some justification for unit conversion is needed in the equation. The M_x is the molecular weight of species x. The $[(x)]$ represents the dissolved gas x. For instance, $[(x)]$ is the sum of $[NH_3(aq)]$ and $[NH_4^+]$ for gaseous NH_3, and the above two states of NH_3 in the aqueous phase can be expressed by Henry's law coefficient and equilibrium constant based on Henry's law and Eq. (2). Therefore, for instance, the gaseous concentration of NH_3 in Eq. (2) is replaced by the following relationship:

$$p_{NH_3} = \frac{p^0_{NH_3} + \frac{q_{NH_3}}{M_{NH_3}} RT}{1 + (K_{ha} + \frac{K_{ha}K_{a1}}{K_w}[H^+])LRT}\ . \quad (17)$$

Similarly, the other gaseous concentrations can be modified as follows.

$$p_{HCl} = \frac{p^0_{HCl} + \frac{q_{HCl}}{M_{HCl}} RT}{1 + (K_{hl} + \frac{K_{hl}K_{l1}}{[H^+]})LRT}\ , \quad (18)$$

$$p_{HNO_3} = \frac{p^0_{HNO_3} + \frac{q_{HNO_3}}{M_{HNO_3}} RT}{1 + (K_{hn} + \frac{K_{hn}K_{n1}}{[H^+]})LRT}, \quad (19)$$

$$p_{CO_2} = \frac{p^0_{CO_2} + \frac{q_{CO_2}}{M_{CO2}} RT}{1 + (K_{hc} + \frac{K_{hc}K_{c1}}{[H^+]} + \frac{K_{hc}K_{c1}K_{c2}}{[H^+]^2})LRT}, \quad (20)$$

$$p_{SO_2} = \frac{p^0_{SO_2} - [\text{S(IV) oxidized}]LRT}{1 + (K_{hs} + \frac{K_{hs}K_{s1}}{[H^+]} + \frac{K_{hs}K_{s1}K_{s2}}{[H^+]^2})LRT}, \quad (21)$$

$$p_{H_2O_2} = \frac{p^0_{H_2O_2} - [H_2O_2 \text{ consumed for oxidation of S(IV)}]LRT}{1 + K_{hh}LRT}, \quad (22)$$

and

$$p_{O3} = \frac{p^0_{O_3} - [O_3 \text{ consumed for oxidation of S(IV)}]LRT}{1 + K_{ho}LRT}. \quad (23)$$

In Eqs. (17)-(20), the partial pressures of NH_3, CO_2, HCl and HNO_3 gases contain the information regarding the mass loading of ammonium, carbonate, chloride and nitrate aerosols. The above aerosols will dissolve in cloud droplets and produce small amounts of their gaseous phase. Therefore, clouds can act to convert aerosol particles to trace gases (Walcek and Taylor, 1986).

2.3 Modeling of Acidity in Individual Cloud Droplets

In the above subsections , the cloud water acidity is modeled for both open and closed systems. The pH values are obtained by assuming all cloud droplets of an equal size. However, the solute concentration in individual cloud droplets is dependent upon the cloud formation and growth processes, resulting in the dependence of droplet acidity upon the droplet size.

In order to model the acidity in individual cloud droplets, in Eq. (10), the coefficients A, B, C and D are rewritten by adding the subscript j, representing the cloud droplet of radius r_j. Considering the equilibrium between gaseous and aqueous phases in individual cloud droplets, the Eq. (16) can be rewritten as follows:

$$p^0_x + \frac{q_x RT}{M_x} = p_x + \sum_{j=1}^{m} [(x)_j] n(r_j) L_j RT, \quad (24)$$

where L_j is the individual LWC for the droplet of radius r_j. Any terms associated with LRT are rewritten as the sum of the contributions of individual cloud droplets. For instance, Eq. (17) is rewritten as follows:

$$p_{NH_3} = \frac{p^0_{NH_3} + \frac{q_{NH_3}}{M_{NH_3}} RT}{1 + K_{ha} \sum_{j=1}^{m} n(r_j) L_j RT + \frac{K_{ha} K_{a1}}{K_w} \sum_{j=1}^{m} [H^+]_j n(r_j) L_j RT}, \quad (25)$$

where the subscript j denotes the cloud droplet size category of r_j. The relationships for other gases are also modified following the above principle. As a result, the above equation is expanded into m equations for a cloud droplet size distribution which is categorized into m classes. For example, m is 25 for a given cloud droplet size distribution. These 25 sets of equations are simultaneously solved using the iteration method with the least square error within 0.1%.

3. EXPERIMENTAL SETUP

The experimental site is located at Mt. Mitchell (35°44′05″N, 82°17′15″W), North Carolina, the highest peak (2,038 m MSL) in the eastern USA. An observation tower of 16.5 m extending about 10 m above the Fraser fir trees, was fully instrumented with meteorological sensors. The microphysical instruments were mounted at the top of the tower. The cloud water and cloud droplet size distributions were concurrently measured during the 1987 field season. The cloudwater was collected using a California Institute of Technology active-cloud-water collector (Jacob *et al.*, 1985). The collected cloud water was delivered via a teflon tube to a Cloud and Rain Acidity/Conductivity analyzer (CRAC, see Paur, 1987) for a real-time measurement of cloud water acidity and also for storage of the samples for later chemical analysis when the amount of collected cloudwater accumulated to 50 ml. This amount of cloudwater may represent a sampling time of about 5-10 min. A detailed description regarding this collecting system may be found elsewhere (see Aneja *et al.*, 1990). The cloud droplet size distributions were detected using a Forward Scattering Spectrometer Probe (FSSP, see Dye and Baumgardner, 1984). The cloud liquid water content was also computed by integrating the cloud droplet distribution. The details of the experimental setup can be found in Saxena *et al.* (1989) and Saxena and Lin (1990).

4. RESULTS AND DISCUSSION

4.1 Model Simulation of Cloudwater Acidity

In order to test the cloud chemistry model, the temperature and liquid water content are assumed to be constant (288 K and 0.5 g m^{-3}, respectively) and the air parcel is assumed to be a closed system without mass exchange with the surrounding environment in most cases. The initial conditions for the gaseous and aerosol concentrations for 10 cases are listed in Table 5.

The oxidation of SO_2 by H_2O_2 and O_3 is investigated in Cases 1-3. In Figure 1 is shown the time variation of the pH values, the sulfate ion concentrations produced by the oxidation of S(IV). The curve for the pH value sharply drops from 4.89 to below 3.8 after about 5 min of reaction time, as shown in Figure 1(a). In contrast, concentration of sulfate ions goes up to more than 80 μM. It is found that about 10% of SO_2 is dissolved into the cloud droplets when H_2O_2 is almost consumed for the oxidation of S(IV). Only about 2%

Table 5. The initial condition for the simulation of acqueous phase chemistry in cloudwater.

Case	1	2[a]	4	5	6	7	8[b]	10
Gas concentration (ppb)								
CO_2 (ppm)	320	320	320	320	320	320	320	320
NH_3		1	1	1	1	1	1	1
SO_2	10	10	10	10	10	10	10	10
HNO_3		1	1	1	1	1	1	1
HCl		1	1	1	1	1	1	1
H_2O_2	1	1	1	1	1	1	1	1
O_3	50	50	50	50	50	50	50	50
Aerosol loading ($\mu g\ m^{-3}$)								
H_2SO_4			2				2	2
$(NH_4)_2SO_4$				2			2	2
NH_4NO_3				2			2	2
NaCl					2		2	2
KCl					2		2	2
$CaCO_3$						2	2	2
$MgCO_3$						2	2	2
Meteorological parameters								
T (K)	288	288	288	288	288	288	288	288
LWC ($g\ m^{-3}$)	0.5	0.5	0.5	0.5	0.5	0.5	0.5	0.1-1.1

a. Case 3 is the same as Case 2 but H_2O_2 and O_3 are remained in constant.
b. Case 9 is the same as Case 8 but H_2O_2 and O_3 are remained in constant.

of O_3 is involved into the oxidation of S(IV). The pH value and sulfate ion concentration almost remain constant when the concentration of H_2O_2 drops to near zero. It is evident that the oxidation of S(IV) is primarily accomplished by H_2O_2. Cases 2 and 3 include the same gases but for Case 3 the entrainment of the H_2O_2 and O_3 is allowed. As a result, more than 95% of the SO_2 is oxidized by entrained H_2O_2 and O_3 after 30 min of reaction time in Case 3, as shown in Figure 2. When the SO_2 is almost oxidized, the sulfate ion concentration in Case 3 is more than four times that in Case 2. The final pH value in Case 3 is about 3.2 and is lower by 0.5 unit when compared with Case 2. Entrainment of pollutants seems to significantly modify the cloud water acidity.

In Cases 4-7 we explored (see Table 5) the influences of scavenged aerosols on the cloud water acidity, including the acidic (H_2SO_4), neutral ($(NH_4)_2SO_4$ and NH_4NO_3), maritime (NaCl and KCl), and continental ($CaCO_3$ and $MgCO_3$) aerosols. The results are shown in Figure 3. The sulfate and nitrate aerosols are major contributors to the cloud water acidity. Carbonate aerosols increase the pH value when they are just scavenged by cloud droplets. However, increased sulfate ions by the oxidation of S(IV) offset the above effect of carbonate loadings. The neutralized ammonium sulfate and nitrate aerosols reveal the moderate effect of acidifying the cloud water. In Figure 3(b), the sulfate ion production for Case 7 is slightly

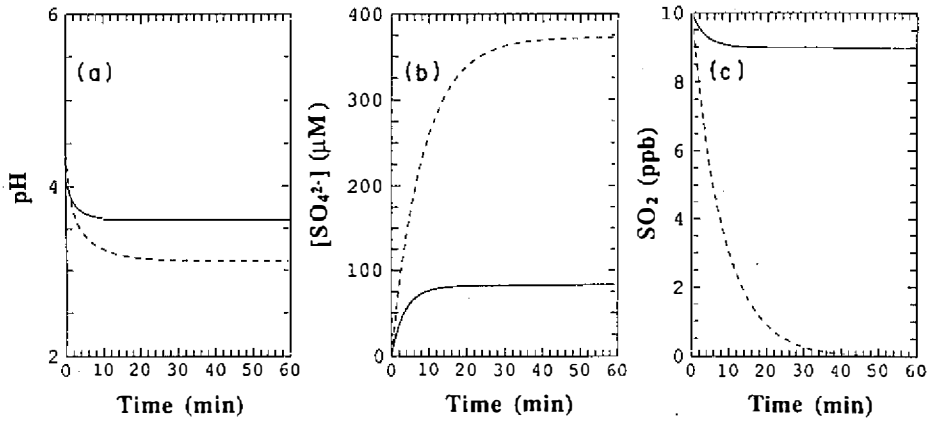

Fig. 1. The simulation results of Case 1. (a) pH value, (b) sulfate ion concentration, and (c) concentrations of SO_2 (annotated as 1), H_2O_2 (annotated as 2) and O_3 (annotated as 3) remaining in the air.

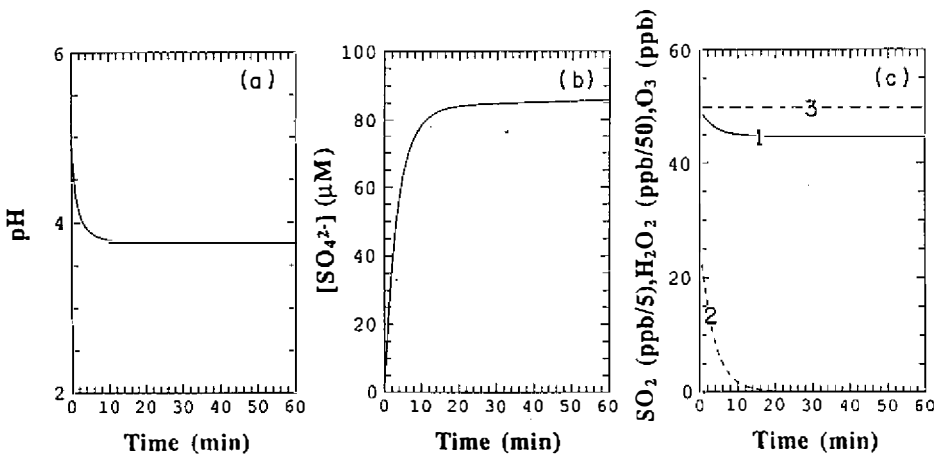

Fig. 2. Comparison of Cases 2 (solid line) and 3 (dashed line). (a) pH value, (b) sulfate ion concentration, and (c) SO_2 remaining in the air.

higher than that in Case 5. This is because the oxidation rate of S(IV) by O_3 at pH=5 is more than 10 times that at pH=4. More sulfate ions are produced when carbonate aerosols are just scavenged by the cloud droplets and increase the pH value to about 5.5 in Case 7. The results of Case 6 for sea salt aerosols are not included in Figure 3. The sodium and potassium chlorides are neutral. When they are scavenged by the cloud droplets, the chloride aerosols can be converted to HCl gas. However, the converted amount is extremely small due to the very large Henry's law coefficient of HCl which is of the order of 10^3 M atm^{-1}.

As shown in Figure 4, the comparison of Cases 8 and 9 is similar to that of Cases 2 and 3, but the former includes the scavenging of aerosol particles (Table 5). The difference in the pH values for Cases 8 and 9 is significantly larger than that for Cases 2 and 3, resulting

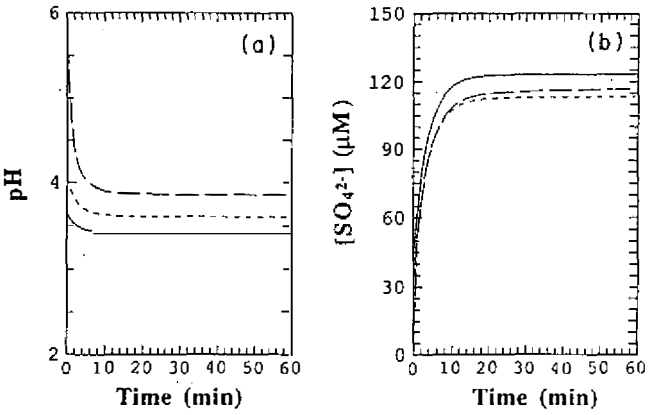

Fig. 3. Comparison of Cases 4 (solid line), 5 (dashed line) and 7 (broken line). (a) pH value, (b) sulfate ion concentration.

from the addition of ammonium and carbonate aerosols in the former cases. The higher sulfate ion concentrations illustrated in Figure 4 as compared to those in Figure 2 are due to sulfate loadings.

To investigate the dependence of cloud water acidity upon cloud liquid water content (LWC), Case 10 is run for the LWC from 0.1 to 1.1 g m^{-3} with a 0.2 g m^{-3} increment. In Figure 5 are shown the pH value and sulfate ion concentration as functions of LWC after the reaction time of 10 min. The dilution effect of the cloud water can be seen in Figure 5(a) in which the pH value for LWC = 1.1 g m^{-3} is about one unit higher than that for LWC = 0.1 g m^{-3}. For the latter, the pH value is even below 3.0. It is noteworthy that the sulfate ion concentration dramatically drops from about 750 to 225 μM as the LWC varies from 0.1 to 0.3 g m^{-3}.

4.2 Dependence of Cloudwater Acidity upon Cloud Droplet Size

In the previous subsections , the cloud water acidity has been modeled for both open and closed systems. The input LWC is a measure of the total mass (in g) of all cloud droplets in a unit volume (in m^3). Therefore, in the cloud chemistry model, the pH values are obtained by assuming all cloud droplets to be of equal size. However, the solute concentration in individual cloud droplets is dependent upon the cloud formation and growth processes, resulting in the dependence of droplet acidity upon droplet size. Modeling the acidity in individual cloud droplets involves large uncertainties and difficulties in properly describing the dynamic growth of such cloud droplets and the chemical reactions involved. In this subsection, the acidity and chemical compositions of individual cloud droplets are modeled based on the cloud chemistry model developed in the preceding subsections.

Theoretical studies (Hegg and Hobbs, 1979; Jensen and Charlson, 1984) have found that total solute mass concentration is smaller inside the smaller drops when nucleation scavenging is the controlling process. In contrast, Flossmann *et al.* (1985) suggested that the mass mixing ratio of aerosols is larger inside smaller drops when condensation and collision-coalescence are the dominant processes. Noone *et al.* (1988) observed that the mean solute concentration in cloud droplets of 9-18 μm sampled from a maritime stratus cloud is a factor of 2.7 smaller

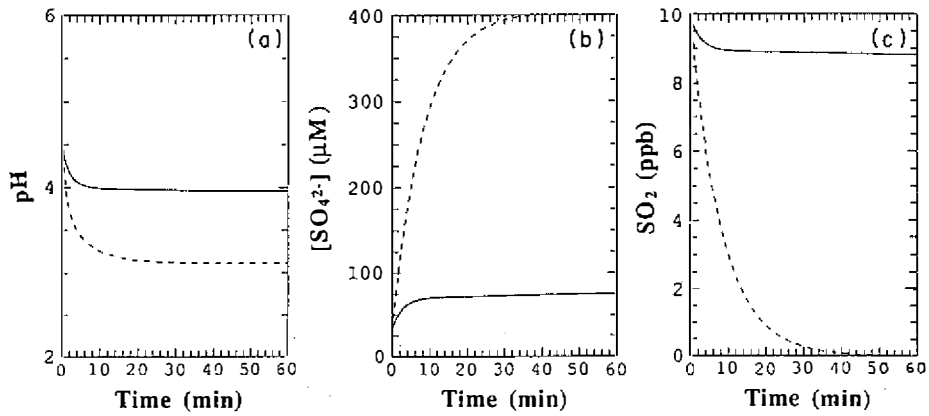

Fig. 4. Comparison of Cases 8 (solid line) and 9 (dashed line). (a) pH value, (b) sulfate ion concentration, and (c) SO_2 remaining in the air.

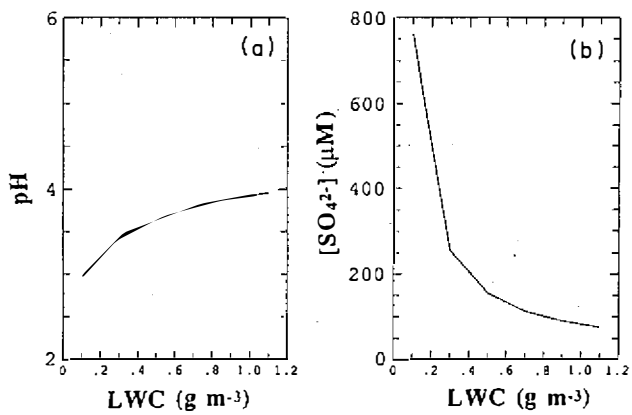

Fig. 5. The effect of cloud liquid water content (LWC) in cloud chemistry. (a) pH value and (b) sulfate ion concentration as a function of LWC at reaction time of 10 min, assuming the same initial condition as that of Case 8.

than that of cloud droplets of 18-23 μm. The dynamics of cloud formation and growth processes strongly influence the solute concentration in cloud droplets. In this study, the aerosols are assumed to be completely incorporated into cloud droplets by either nucleation or impaction scavenging regardless of their loadings. No dynamic growth of cloud droplets is considered.

The cloud droplet size distributions measured by FSSP at the Mitchell site (Saxena *et al.*, 1989; DeFelice, 1990) were found to be well described by the Khrgian-Mazin droplet size distribution (see Pruppacher and Klett, 1980) as follows,

$$n(r) = Pr^2 \exp(-Qr), \tag{26}$$

where $n(r)dr$ represents the number concentration of droplets in the radius range $(r, r+dr)$.

The parameters P and Q can be related to any two moments of the distribution. In terms of the total concentration N and the average radius $\bar{r}$, then,

$$N = \int_0^\infty n(r)dr = \frac{2p}{Q^3}, \tag{27}$$

and

$$\bar{r} = \frac{1}{N}\int_0^\infty n(r)dr = \frac{3}{Q}. \tag{28}$$

The liquid water content of the cloud can be expressed as follows.

$$\text{LWC (g m}^{-3}) = 10^6(4/3)\rho_w \int_0^\infty r^3 n(r)dr, \tag{29}$$

where ρ_w is the density of water in g cm^{-3} and r is in cm. For such a distribution one can find the following approximate values,

$$P = 1.45 \times 10^{-6}(\text{ LWC }/\rho_w \bar{r}^6), \tag{30}$$

and

$$N = 1.07 \times 10^{-7}(\text{ LWC }/\rho_w \bar{r}^3). \tag{31}$$

Given the average droplet size and liquid water content, the corresponding parameters P and Q for the Khrgian-Mazin droplet size distribution can be obtained, and therein, Eq. (26) can be integrated on a specified range of droplet size (r_1, r_2) and after integration,

$$N(r_1, r_2) = \frac{P}{Q}e^{-Q}(r^2 + \frac{2}{Q}r + \frac{2}{Q^2})|_{r=r_2}^{r=r_1}. \tag{32}$$

By means of Eq. (32), the cloud droplet size spectra with respect to 5 liquid water content classes (0.1, 0.3, 0.5, 0.7 and 1.0 g m^{-3}) and 25 droplet size categories are evaluated. The results are shown in Figure 6, predictably revealing that the modal droplet radius becomes larger as liquid water content increases, but the higher droplet concentration corresponds to the lower liquid water content class.

The solute mass in each cloud droplet for species x is assumed to be proportional to the radius of the cloud droplet. Thus, the mixing ratio $w_{x,r}(\mu\text{g g}^{-1})$ of solute mass to the mass of the cloud droplet of radius r can be expressed as follows:

$$w_{x,r} = \frac{q_x r}{(4/3\pi r^3 \rho_w)\sum_{j=1}^{m} r_j n(r_j)}. \tag{33}$$

Using the above described Khrgian-Mazin droplet size distribution, the mixing ratios for liquid water content ranging from 0.1 to 1.0 g m^{-3} can be calculated as a function of droplet sizes. For simplicity, the microphysical processes between the cloud droplets are ignored. The cloud droplet size distribution is assumed to be steady during the model simulation (about 10 min).

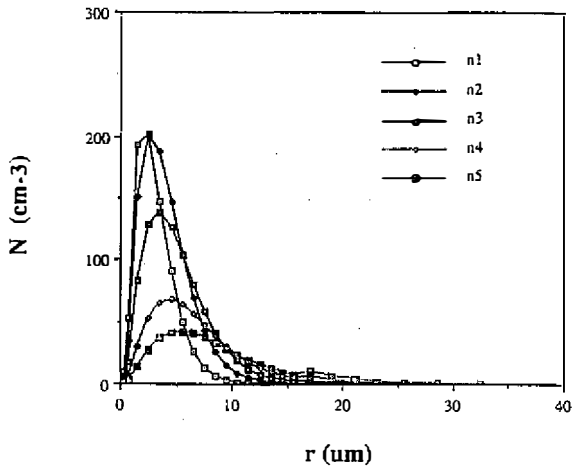

Fig. 6. Khrgian-Mazin droplet size distributions at five LWC classes (n1-n5 represent the LWC values of 0.1, 0.3, 0.5, 0.7 and 1.0 g m^{-3}, respectively.), used for simulating the acidity in individual cloud droplets.

In order to test the dependency of the cloud droplet acidity on its size, the corresponding cloud droplet size distribution for liquid water content of 0.5 g m^{-3} is used as a representative distribution. The initial condition is assumed the same as that for Case 8 (shown in Table 5). As a result, smaller droplets have higher pH values (i.e. less acidic) although the sulfate ion concentrations in them are much higher than in larger droplets, as seen in Figure 7(a). When the droplet sizes are greater than 2.5 μm, the variation of pH values with droplet sizes is not significant. Contrary to conventional behavior, the solid-line curve exhibits less acidity for smaller droplets. This is a consequence of the neutralizing capacity of carbonate aerosols.

Once the latter is exhausted, the acidic aerosols are responsible for producing stronger acidic content (lower pH values) as the droplet size increases. The model simulation is also performed for the case in which the carbonate aerosols are excluded. As seen in Figure 7(a), the result is opposite to the previous one of full inputs. When the droplet sizes are greater than 1.5 μm, the pH values change within only 0.2 unit. The smaller droplets have higher acidity.

By comparing the above two cases, the smaller droplets are found to be most sensitive to aerosol loadings, primarily resulting from their smaller volumes. Although the larger droplets are assumed to have more aerosols dissolved, their resulting pH values are not sensitive to variation in droplet sizes. In Figure 7(b) are shown the sulfate ion concentrations produced in these two cases. It is found that the concentrations in the case of full inputs (Case 8 in Table 5) are only slightly higher than that in the other case for those droplets of larger than 3.5 μm. In contrast, the sulfate ion concentration differs by a factor of two for the smallest droplet. The pH value for the smallest droplet in the case of full inputs is about 4.3 unit lower than that in the other case. The dilution effect in larger droplets can be seen in these model simulations. The carbonate aerosols significantly neutralize the acid aerosols in the case of full inputs. The sulfate and nitrate aerosols are the dominant species to acidify the cloud droplets, especially for the smallest droplet.

In the above case of no carbonates, the volume-weighed pH value over the cloud droplet size distribution is 3.40. The bulk pH value as calculated in Case 8 is at the same level, but

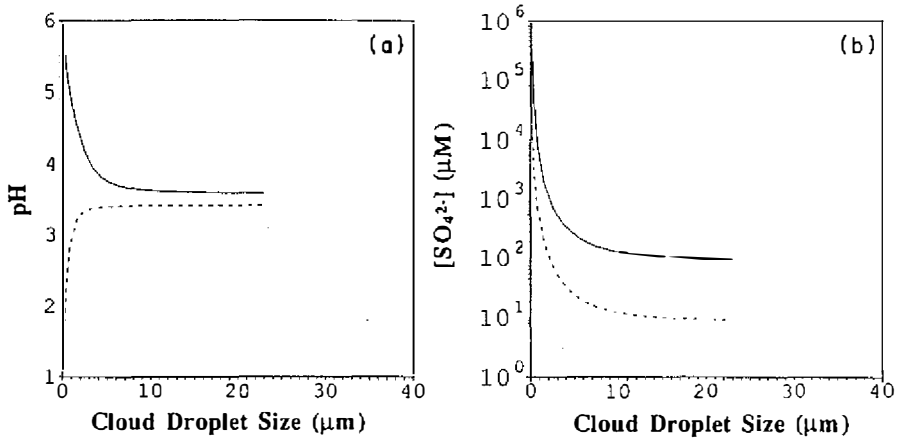

Fig. 7. The dependence of the acidity of cloud droplets upon their sizes. Comparison of the model simulations for the following conditions: (1) full inputs (same as that of Case 8), and (2) excluding the carbonate aerosols. Solid and dashed lines represent the former and latter, respectively. (a) pH values and (b) sulfate ion concentrations as a function of cloud droplet size. In (b), the sulfate concentration for condition (2) is reduced by a factor of 10 in order to differ from condition (1).

slightly larger than the volume-weighed one. However, when the solute mass is assumed to be proportional to r^2 and r^3 (see Eq. (33)), the volume-weighed pH values go up to 3.42 and 3.43, respectively.

For the full model inputs, the simulations are further performed for five LWC classes as described previously. The results are shown in Figure 8. In general, the higher the liquid water content, the smaller the acidity in cloud droplets (Line 1 in Figure 8). For the case of the lowest liquid water content, the acidity is significantly higher than those for other cases. However, the acidity in cloud droplets may not be a linear function of the liquid water content, as seen in the case (Line 3) of LWC = 0.5 g m^{-3}. The cloud droplet size distribution is another factor to influence the cloud droplet acidity, because the mixing ratio of aerosols in cloud droplets is strongly dependent upon their sizes. Lines 2 and 4 in Figure 8 have almost identical dependence of pH and sulfate ion concentration upon the droplet radius, although the corresponding LWC values are 0.3 and 0.7 g m^{-3}, respectively. The corresponding size distributions (n2 and n4 in Figure 6) are also different.

4.3 Comparison with Experimental Results

For comparison between model simulations and experimental results, the cloud microphysical, dynamic and chemical features during a cloud event of August 19, 1987 observed at Mt. Mitchell, NC, are studied. In Figure 9 are shown the mean sizes of cloud droplet size distributions measured (DeFelice and Saxena, 1990) by a Forward Scattering Spectrum Probe (FSSP), cloud liquid water content, sulfate and nitrate ion concentrations and the corresponding pH values detected (Kim and Aneja, 1992) by a real-time cloud/rain and conductivity analyzer.

In Figure 9 is shown a time series for four observed parameters: (a) mean cloud droplet size, (b) liquid water content (LWC), (c) concentration of sulfate and nitrate ions, and (d)

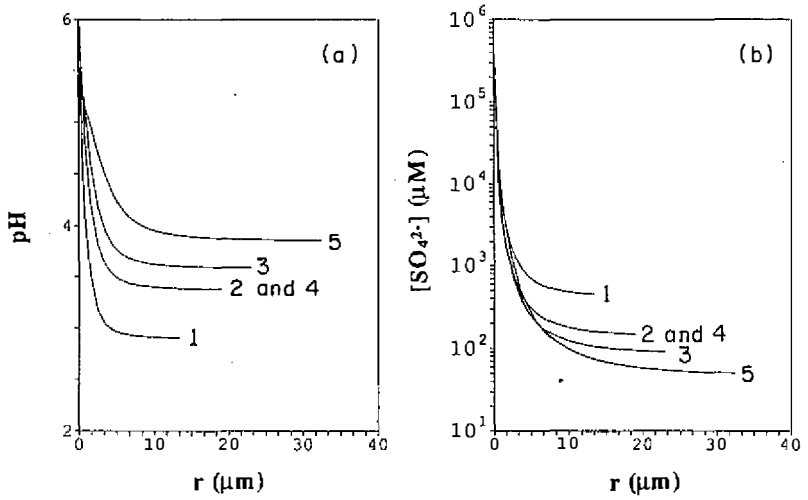

Fig. 8. (a) pH value, (b) sulfate ion concentration as a function of cloud droplet size at five LWC classes (which are annotated by 1-5, respectively) as shown in Fig. 6. The initial condition is the same as that of Case 8.

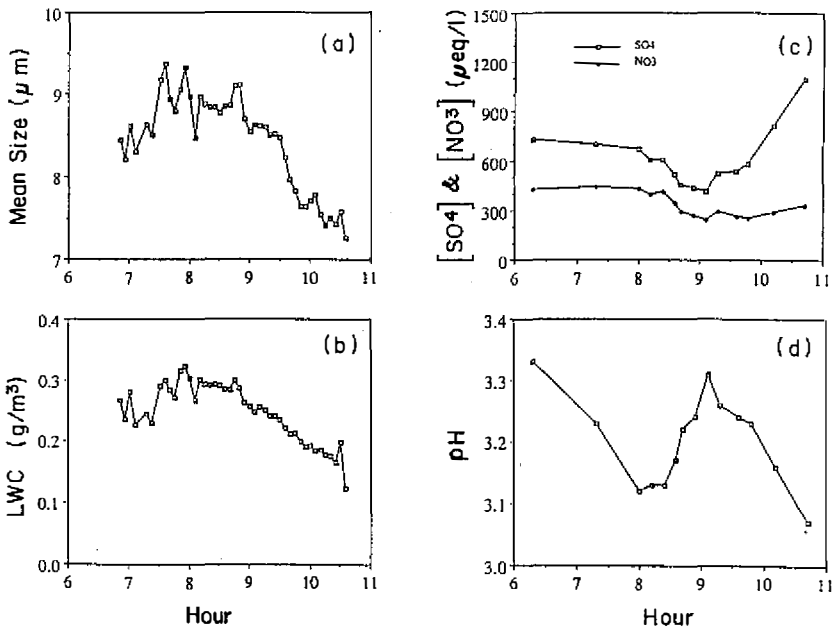

Fig. 9. The cloud micro physical parameters and cloudwater chemistry measured at the Mt. Mitchell site during the cloud event of August 19, 1987. (a) Mean size, (b) LWC, (c) sulfate and nitrate ion concentrations and (d) pH value of cloud droplets.

real-time observations of pH of cloud water – an indicator of the acidity of cloud droplets. As pointed out by DeFelice and Saxena (1990), the prevailing winds producing this cloud event were from WNW and were conducive to bringing continental aerosols (such as $CaCO_3$ and $MgCO_3$) to the site. After the onset of the cloud event, the pH of cloud droplets (Figure 9d) decreased during the first two hours, and so did the concentrations of sulfate and nitrate ions, although the mean cloud droplet size and liquid water content increased during the same period of time, suggesting the diffusional/condensational growth of cloud droplets during formative stages. The decrease in pH is similar to the model results displayed in Figure 7(a) represented by the solid-line curve. The observed dependency of sulfate ion concentration (Figure 9c) upon droplet size follows the trend displayed in Figure 7(b). This qualitative agreement with the model results is indeed encouraging since it lends support to the assumptions upon which the model is based. It also indicates that the model could be used as an effective diagnostic tool for realistic assessment of the cloud water acidity and analysis of its dependence upon the droplet size.

Upon reaching a minimum pH after two hours (Figure 9d), the acidity of cloud droplets decreased (pH increased) as the mean cloud droplet size (Figure 9a) and the liquid water content (Figure 9b) increased. This trend is the result of the condensational growth process that continues after the neutralizing capacity of continental aerosols is exhausted as shown by the broken line curve in Figure 7(a). During its dissipative stages, the cloud entrained surrounding dry and polluted air. Consequently, the mean droplet size and LWC decreased with simultaneous increase in sulfate ion concentration. This lowers the pH of evaporating cloud droplets as shown in Figure 9(d). The observed variation of pH of cloud droplets with their sizes is thus in qualitative agreement with the model results. This modeling study can help identify and quantify the effect of individual chemical processes on the acidity of cloud droplets when these have achieved a state of chemical equilibrium.

5. CONCLUDING REMARKS

A cloud chemistry model (CCM) has been developed as a diagnostic tool to assess acidity of cloud water under varying conditions of aerosol and gaseous-precursor loading. The solution chemistry involves SO_2, HNO_3, HCl, NH_3, CO_2, O_3 and H_2O_2 gases and the oxidation of S(IV) by O_3 and H_2O_2. The model includes the scavenging of acidic (H_2SO_4), neutral ($(NH_4)_2SO_4$ and NH_4NO_3), maritime (NaCl and KCl), and continental ($CaCO_3$ and $MgCO_3$) aerosols. A scheme is developed for investigating the dependence of the acidity and chemical composition in cloud droplets upon their sizes.

The results of this study indicate that

- about 10% of gaseous SO_2 is in general consumed for producing the S(IV) and the sulfate ions,
- the addition of aerosols strongly affects the acidity of cloud droplets, the effect being strongest in smallest droplets,
- the scavenging of sulfate and nitrate aerosols is the most efficient mechanism to acidify the cloud water.

Qualitative agreement is also found between direct observations of the trend in pH variation with the droplet size and the model predictions. Although in its present form the model does not include the dynamics of clouds, it is feasible to link the developed model with a dynamic cloud model.

Acknowledgments This study is supported through the National Science Council of Taiwan under contract No. NSC-82-0202-M-008-110 and NSC-83-0202-M-008-039. Prof. V. K. Saxena gave some suggestions. Prof. T. P. DeFelice provided the FSSP data and Dr. D. S. Kim operated the CRAC analyzer. Valuable comments from the reviewers are highly appreciated.

REFERENCES

Aneja, V. P., C. S. Claiborn, and R. L. Bradow, 1990: Dynamic chemical characterization of montane clouds. *Atmos. Environ.*, **24A**, 563-572.

Beilke, S., and G. Gravenhorst, 1978: Heterogeneous SO_2 oxidation in the droplet phase. *Atmos. Environ.*, **12**, 231-239.

Chen, C. C., H. I. Britt, J. F. Boston, and L. B. Evans, 1979: Extension and application of the Pitzer equation for vapor liquid equilibrium of aqueous electrolyte systems with molecular solutes. *Am. Inst. Chem. Eng. J.*, **25**, 820-831.

Cruz, J.-L., and H. Rennon, 1978: A new thermodynamic representation of binary electrolyte solutions nonideality in the whole range of concentrations. *Am. Inst. Chem. Eng. J.*, **24**, 871.

DeFelice, T. P., and V. K. Saxena, 1990: Temporal and vertical distribution of acidity and ionic composition in clouds: comparison between modeling results and observations. *J. Atmos. Sci.*, **47**, 1117-1126.

Dye, J. E., and D. Baumgardner, 1984: Evaluation of the Forward Scattering Spectrometer Probe, Pt. I: Electronic and optical studies. *J. Atmos. and Oceanic Tech.*, **1**, 329-344.

Easter, R. C., and D. J. Luecken, 1988: A simulation of sulfur wet deposition and its dependence on the inflow of sulfur species to storms. *Atmos. Environ.*, **22**, 2715-2739.

Erickson, R. E., L. M. Yates, R. L. Clark, and D. McEwen, 1977: The reaction of sulfur dioxide with ozone in water and its possible atmospheric significance. *Atmos. Environ.*, **11**, 813-817.

Flossmann, A. E., W. D. Hall, and H. R. Pruppacher, 1985: A theoretical study of wet removal of atmospheric pollutants. Pt. I: the redistribution of aerosol particles captured through nucleation and impaction scavenging by growing cloud drops. *J. Atmos. Sci.*, **42**, 583-606.

Hales, J. M., and D. R. Drewes, 1979: Solubility of SO_2 in water at low concentrations. *Atmos. Environ.*, **13**, 1133-1147.

Hales, J. M., and S. L. Sutter, 1973: Solubility of ammonia in water at low concentrations. *Atmos. Environ.*, **7**, 997-1001.

Harned, H. S., and R. Davis, 1943: The ionization constant of carbonic acid and the solubility of carbon dioxide in water and aqueous salt solutions from 0 to 500. *J. Am. Chem. Soc.*, **65**, 2030-2037.

Hegg, D. A., and P. V. Hobbs, 1979: The homogeneous oxidation of sulfur dioxide in cloud droplets. *Atmos. Environ.*, **13**, 981-987.

Heggs, D. A. ,and T. V. Larson, 1990: The effects of microphysical parameterization on model predictions of sulfate production in clouds. *Tellus*, **42B**, 272-284.

Heintzenberg, J., 1992: The Po Valley Fog Experiment 1989. What have we learned, where do we go from here? *Tellus*, **44B**, 443-447.

Jacob, D. J., J. M. Waldman, M. Haghi, M. J. Hoffmann, and R. C. Flagan, 1985: An instrument to collect fogwater for chemical analysis. *Rev. Sci. Instrum.*, **56**, 1291-1293.

Jensen, J. B., and R. J. Charlson, 1984: On the efficiency of nucleation scavenging. *Tellus*, **36B**, 367-375.

Johnstone, H. F., and P. W. Leppla, 1934: The solubility of SO_2 at low partial pressure: the ionization constant and heat of ionization of sulfurous acid. *J. Am. Chem. Soc.*, **56**, 2233-2238.

Lee, I.-Y., 1983: Formation of sulfates in cloud-free environment. *J. Clim. Appl. Meteor.*, **22**, 163-170.

Lee, I.-Y., 1986: Numerical simulation of chemical and physical properties of cumulus clouds. *Atmos. Environ.*, **20**, 767-771.

Lin, N.-H., and V. K. Saxena, 1991a: Interannual variability in acidic deposition on the Mt. Mitchell area forest. *Atmos. Environ.*, **25A**, 517-524.

Lin, N.-H., and V. K. Saxena, 1991b: In-cloud scavenging and deposition of sulfates and nitrates: case studies and parameterization. *Atmos. Environ.*, **25A**, 2301-2320.

Martin, L. R., and D. E. Damschen, 1981: Aqueous oxidation of SO_2 by H_2O_2 at low pH. *Atmos. Environ.*, **15**, 1615-1621.

Noone, K. J., R. J. Charlson, D. S. Covert, J. A. Ogren, and J. Heintzenburg, 1988: Cloud droplets: solute concentration is size dependent. *J. Geophys. Res.*, **93**, 9477-9482.

Ogren, J. A., K. J. Noone, A. Hallberg, J. Heintzenberg, D. Schell, A. Berner, L. Solly, C. Kruisz, G. Reischl, B. G. Arends, and W. Wobrock, 1992: Measurements of the size dependence of the concentration of non-volatile material in fog droplets. *Tellus*, **44B**, 570-580.

Paur, R. J., 1987: Project summary: development and evaluation of a real-time pH and conductivity rain monitor. EPA-600/54-87/010. USEPA, Research Triangle Park, NC.

Pandis, S., and J. H. Seinfeld, 1990: Chemical composition differences in fog and cloud droplets of different sizes. *Atmos. Environ.*, **24A**, 1957-1969.

Pruppacher, H. R., and J. D. Klett, 1980: Microphysics of Clouds and Precipitation. Reidel, Boston, 714pp.

Saxena, V. K., and N.-H. Lin, 1990: Cloud chemistry measurements and estimates of acidic deposition on an above cloudbase coniferous forest. *Atmos. Environ.*, **24A**, 329-352.

Saxena, V. K., R. E. Stogner, A. H. Hendler, T. P. DeFelice, R. J.-Y. Yeh, and N.-H. Lin, 1989: Monitoring the chemical climate of the Mt. Mitchell State Park for evaluating its impaction on forest decline. *Tellus*, **41B**, 92-109.

Schwartz, S. E., and W. H. White, 1981: Solubility equilibria of the nitrogen oxides and oxy-acids in dilute aqueous solution. In Advanced in Environmental Science and Engineering. Pfafflin J. R. and Ziegler E. N. (Eds.). Gordon and Breach, New York.

Schwartz, S. E., 1984: Gas-aqueous reactions of sulfur and nitrogen oxides in liquid water clouds. In SO_2, NO and NO_2 Oxidation Mechanisms. Calvert J. G. (Ed.), Butterworth publisher, Boston, 254pp.

Wagman, D. D., W. H. Evans, V. B. Parker, L. Halow, S. M. Bailey, and R. H. Schumm, 1968: Selected values of chemical thermodynamic properties. In Tables for the First Thirty-Four Elements in the Standard Order of Arrangement. US NBS Technical Note 270-3, National Bureau of Standards, US Department of Commerce, Washington, D.C.

Walcek, C. J., and G. R. Taylor, 1986: A theoretical method for computing vertical distributions of acidity and sulfate production with cumulus clouds. *J. Atmos. Sci.*, **43**, 339-355.

Weast, R. C., 1984: CRC Handbook of Chemistry and Physics. CRC Press, Boca Raton, FL.